PHYSICAL REVIEW D **87,** 075025 (2013)

Electroweak corrections to the direct detection cross section of inert Higgs dark matter

Michael Klasen* and Carlos E. Yaguna†
Institut für Theoretische Physik, Universität Münster, Wilhelm-Klemm-Straße 9, D-48149 Münster, Germany

José D. Ruiz-Álvarez‡
Instituto de Física, Universidad de Antioquia, A.A. 1226 Medellín, Colombia
(Received 13 February 2013; published 26 April 2013)

The inert Higgs model is a minimal extension of the Standard Model that features a viable dark matter candidate, the so-called inert Higgs (H^0). In this paper, we compute and analyze the dominant electroweak corrections to the direct detection cross section of dark matter within this model. These corrections arise from one-loop diagrams mediated by gauge bosons that, contrary to the tree-level result, do not depend on the unknown scalar coupling λ. We study in detail these contributions and show that they can modify in a significant way the prediction of the spin-independent direct detection cross section. In both viable regimes of the model, $M_{H^0} < M_W$ and $M_{H^0} \gtrsim 500$ GeV, we find regions where the cross section at one loop is much larger than at tree level. We also demonstrate that, over the entire viable parameter space of this model, these new contributions bring the spin-independent cross section within the reach of future direct detection experiments.

DOI: 10.1103/PhysRevD.87.075025 PACS numbers: 12.60.−i, 95.35.+d, 12.60.Fr

I. INTRODUCTION

Direct detection is possibly the most promising way of observing and identifying the dark matter—that mysterious form of matter that accounts for about 20% of the energy density of the Universe [1]. Direct detection experiments try to observe, via recoil energy, the scattering of dark matter particles with nuclei and to determine from it some fundamental properties of the dark matter particle, such as its mass and its interactions. In recent years, these experiments, particularly XENON100 [2,3], have made outstanding progress in this regard and have started to exclude interesting regions of the parameter space of common models of dark matter—see e.g., Refs. [4–7]. In the near future, planned experiments, such as XENON-1T, will either find direct evidence of dark matter or increase the excluded regions even further. In both cases, it is of crucial importance to have reliable predictions for the direct detection cross section of dark matter. Otherwise, we would not be able to assess the implications of forthcoming data for specific models of dark matter or to foresee the extent to which future facilities would be able to constrain them.

In most dark matter models, the one-loop electroweak contributions to the dark matter direct detection cross section are expected to give only a tiny correction to the tree-level result, so there is no need, at least at present, to compute them. It may happen, however, that the tree-level result features a strong suppression not necessarily present at higher orders. If that is the case, the calculation of such electroweak corrections becomes necessary if one wants to correctly predict the direct detection cross section of dark matter. It turns out that this situation actually arises in one of the most economical models that have been proposed to explain the dark matter puzzle: the inert doublet model [8–10].

In the inert doublet model, the Standard Model is extended with a second Higgs doublet that is odd under a new Z_2 symmetry. The lightest component of this doublet becomes automatically stable and, if neutral, a good dark matter candidate, the so-called inert Higgs (H^0). In recent years, the phenomenology of this model has been extensively studied in a number of works—see e.g., Refs. [11–27]. In the inert doublet model, the tree-level direct detection cross section is determined by a Higgs (h) mediated diagram and will be suppressed whenever the coupling H^0H^0h, which is proportional to a free parameter of this model, becomes small. Since at one loop, H^0q scattering may proceed entirely via gauge processes ($W^\pm$ and Z^0 mediated diagrams), it is not guaranteed that these one-loop corrections will be smaller than the tree-level result. Motivated by this simple observation, we calculate and analyze, in this paper, the dominant electroweak corrections to the direct detection cross section of inert Higgs dark matter. We will see that they may modify in a significant way the tree-level prediction within important regions of the viable parameter space, sometimes giving the dominant contribution to the spin-independent direct detection cross section. Moreover, they always bring this cross section within the reach of future experiments such as XENON-1T.

The rest of the paper is organized as follows. In the next section the inert doublet model of dark matter is briefly reviewed, outlining its parameter space and its viable regions. Then, in Sec. III, we present the calculation of

*michael.klasen@uni-muenster.de
†carlos.yaguna@uni-muenster.de
‡Present address: IPNL, Lyon, France.
jose@gfif.udea.edu.co

the dominant electroweak corrections to the direct detection cross section of inert Higgs dark matter and show its behavior as a function of the parameters of the model. Sections IV and V contain our main results. They demonstrate the impact of these electroweak corrections within the two viable regimes of the model: the low mass one ($M_{H^0} < M_W$) in Sec. IV and the large mass one ($M_{H^0} \gtrsim 500$ GeV) in Sec. V. In both cases, we identify the regions where the corrections are expected to be important. To further substantiate our findings, we perform a scan over the entire parameter space of the model, and we analyze it in some detail. Finally, our conclusions are presented in Sec. VI.

II. THE INERT DOUBLET MODEL

The inert doublet model is a simple extension of the Standard Model with one additional Higgs doublet H_2 and an unbroken Z_2 symmetry, under which H_2 is odd while all other fields are even. This discrete symmetry prevents the direct coupling of H_2 to fermions and, crucial for dark matter, guarantees the stability of the lightest inert particle. The scalar potential of this model is given by

$$V = \mu_1^2|H_1|^2 + \mu_2^2|H_2^2| + \lambda_1|H_1|^4 + \lambda_2|H_2|^4 + \lambda_3|H_1|^2|H_2|^2 + \lambda_4|H_1^\dagger H_2|^2 + \frac{\lambda_5}{2}[(H_1^\dagger H_2)^2 + \text{H.c.}], \tag{1}$$

where H_1 is the Standard Model Higgs doublet, and λ_i and μ_i^2 are real parameters. Four new physical states are obtained in this model: two charged states, $H^\pm$, and two neutral ones, H^0 and A^0. Either of them could account for the dark matter. In the following, we assume that H^0 is the lightest inert particle, $M_{H^0}^2 < M_{A^0}^2$, $M_{H^\pm}^2$, and, consequently, the dark matter candidate. After electroweak symmetry breaking, the inert scalar masses take the following form:

$$\begin{aligned} M_{H^\pm}^2 &= \mu_2^2 + \frac{1}{2}\lambda_3 v^2, \\ M_{H^0}^2 &= \mu_2^2 + \frac{1}{2}(\lambda_3 + \lambda_4 + \lambda_5)v^2, \\ M_{A^0}^2 &= \mu_2^2 + \frac{1}{2}(\lambda_3 + \lambda_4 - \lambda_5)v^2, \end{aligned} \tag{2}$$

where $v = 246$ GeV is the vacuum expectation value of H_1. Let us introduce at this point the parameter λ defined by

$$\lambda \equiv (\lambda_3 + \lambda_4 + \lambda_5)/2. \tag{3}$$

This parameter is of particular relevance to our direct detection study as it determines the coupling H^0H^0h, and therefore the tree-level direct detection cross section—see next section. In addition to λ, it is convenient to take M_{H^0}, M_{A^0}, and $M_{H^\pm}$ as the remaining free parameters of the inert sector. The tree-level direct detection cross section depends also on the Higgs mass (M_h). Given the small range to which M_h has been constrained by recent data [28,29], we have simply set $M_h = 125$ GeV throughout this paper.

The new parameters of the inert doublet model are not entirely free; they are subject to a number of theoretical and experimental constraints—see e.g., Refs. [8,10]. The requirement of vacuum stability imposes that

$$\lambda_1, \lambda_2 > 0, \qquad \lambda_3, \lambda_3 + \lambda_4 - |\lambda_5| > -2\sqrt{\lambda_1\lambda_2}. \tag{4}$$

LEP data constrain the mass of the charged scalar, $M_{H^\pm}$, to be larger than about 90 GeV [30] while some regions in the plane (M_{H^0}, M_{A^0}) are also excluded; see Ref. [12]. In addition, the inert doublet, H_2, contributes to electroweak precision parameters such as S and T, which must be small to remain compatible with current data. Finally, the relic density of inert Higgs dark matter should be compatible with the observed dark matter density [1]. To evaluate Ωh^2, we have used micrOMEGAs [31], which automatically takes into account resonances and coannihilation effects. Into micrOMEGAs we have incorporated the annihilation into the three-body final state WW^* ($H^0H^0 \to WW^* \to Wf\bar{f}'$), which modifies in a significant way the predicted relic density for $M_{H^0} \lesssim M_W$ [20].

In previous works [10,15], it had been found that the dark matter constraint cannot be satisfied for arbitrary values of M_{H^0}. Two separate regions remain viable,[1] one at low masses and the other at large masses. In the low mass regime ($M_{H^0} \lesssim M_W$), the annihilation of dark matter is dominated by either the $b\bar{b}$ final state or the three-body final state WW^*, and may be enhanced due to the presence of the Higgs resonance at $M_{H^0} \sim M_h/2$. Moreover, H^0-A^0 coannihilations may also play a role in the determination of the dark matter relic density. In the large mass regime ($M_{H^0} > 500$ GeV), dark matter annihilates either into gauge bosons (W^+W^-, Z^0Z^0) or into Higgs bosons. These annihilation channels are usually very efficient, so the relic density tends to be suppressed. The observed value of the dark matter density can still be obtained in this regime but only when the mass splitting between the inert particles is tiny. Since these two dark matter compatible regimes have completely different phenomenologies, we will split our analysis and discuss our main results in two different sections, one dedicated to each regime. Before that, we present, in the next section, the calculation of the electroweak corrections to the spin-independent cross section and obtain some preliminary results.

[1]Notice that, as anticipated in Ref. [21], the *new viable region*, $M_W < M_{H^0} \lesssim 150$ GeV, has already been excluded by the recent XENON100 data [2,3].

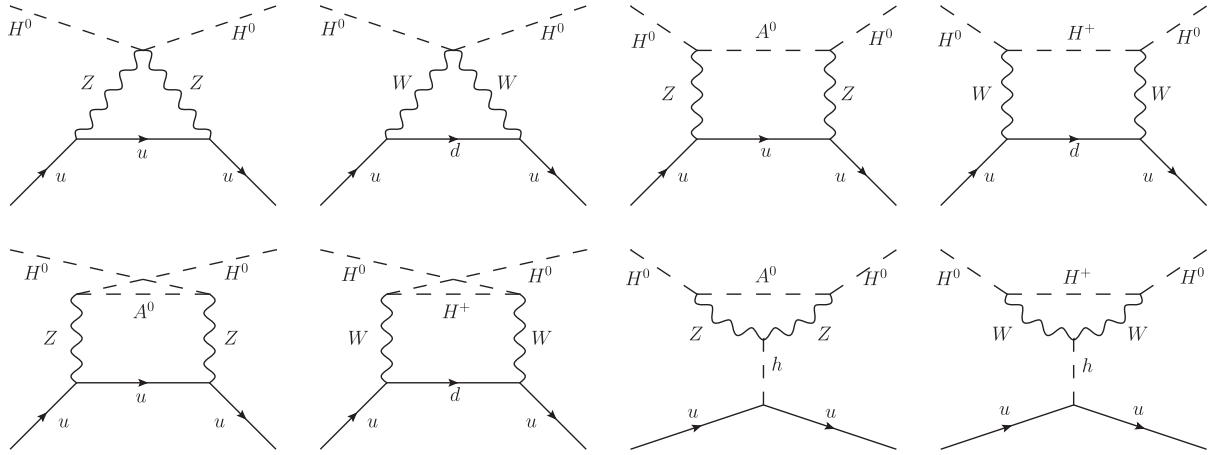

FIG. 1. The Feynman diagrams that give the dominant corrections to the direct detection cross section of inert Higgs dark matter.

III. THE DIRECT DETECTION CROSS SECTION AT ONE LOOP

In the inert doublet model, the dark matter direct detection cross section at tree level is given by

$$\sigma_{\rm SI}(\text{tree level}) = \frac{m_r^2}{\pi}\left(\frac{\lambda}{M_{H^0}M_h^2}\right)^2 f^2 m_N^2, \qquad (5)$$

where f is a quark form factor[2] and m_r is the reduced mass of the dark matter-nucleon system. This cross section arises from a Higgs mediated diagram and is seen to be proportional to λ^2. In many models, the tree-level value of $\sigma_{\rm SI}$ is accurate enough for most purposes and there is no need to compute electroweak corrections to it. The inert doublet model, however, may be an exception to that rule. In fact, in this model not only can the coupling λ be very small (much smaller than the gauge couplings), but there are one-loop diagrams mediated by the gauge bosons that contribute to $\sigma_{\rm SI}$ that do not depend on λ and are instead entirely determined by the gauge couplings and the masses of the inert particles. It is quite possible, therefore, that the tree-level result, Eq. (5), fails to give the correct prediction for the spin-independent direct detection cross section in certain regions of the parameter space. For that reason, in this paper we compute the dominant electroweak corrections to $\sigma_{\rm SI}$, and we analyze their importance in both the low and the large mass regime of the model. A calculation similar to this was first presented in Ref. [32] and later applied to the inert doublet model in Ref. [33]. It must be emphasized, however, that the model in Ref. [32] is not exactly the inert Higgs model and that they considered only the regime $M_{\rm DM} \gg M_W$. Since their results cannot be directly used for our study, we have calculated these corrections ourselves without making any assumptions on the masses of the inert particles. We limit ourselves to those diagrams that might become dominant when λ is small, that is to diagrams mediated by electroweak gauge bosons and independent on λ. The contributing diagrams are shown in Fig. 1. In the following, we denote by $\sigma_{\rm SI}$(tree level) or simply by $\sigma_{\rm SI}$ the value of the spin-independent cross section that is obtained when these diagrams are taken into account. Notice that these electroweak corrections depend only on three unknowns[3]: M_{H^0}, M_{A^0}, and $M_{H^\pm}$. Next, we will numerically study $\sigma_{\rm SI}$ as a function of these parameters, and we will demonstrate that these one-loop contributions may indeed be larger than the tree-level result.

The left panel of Fig. 2 shows the purely one-loop contribution ($\lambda = 0$) to $\sigma_{\rm SI}$ as a function of M_{H^0} for four different values of the mass splitting $\Delta M = M_{A^0}$-$M_{H^0} = M_{H^\pm}$-M_{H^0}. From top to bottom, the lines correspond to $\Delta M = 1$, 10, 20, 50 GeV. Notice that the electroweak corrections give a cross section of order 10^{-11} pb–10^{-10} pb depending slightly on the dark matter mass and on the mass splitting. $\sigma_{\rm SI}$ initially increases with M_{H^0} but then tends to a constant value for large M_{H^0}—a result compatible with that found in Ref. [32]. It is also clear from the figure that $\sigma_{\rm SI}$ decreases with the mass splitting between the inert particles.

One may also wonder what diagrams from Fig. 1 give the dominant contributions to $\sigma_{\rm SI}$. This is illustrated in the right panel of Fig. 2, which displays separately the *gauge* (diagrams 1 to 6, red dash-double-dotted line) and *Higgs* (diagrams 7 and 8, blue dashed line) contributions to $\sigma_{\rm SI}$ as well as the total cross section (red dash-dotted line) for $\Delta M = 1$ GeV. Among the gauge contributions, we have found the boxes (diagrams 3 to 6) to be subdominant but non-negligible with respect to the triangles (diagrams 1 and 2). It is clear from the figure that at low masses the gauge

[2]In our numerical evaluations, we use for the quark form factors f_q the default values from micrOMEGAs [31].

[3]The total amplitude (tree + one loop) will depend also on λ and M_h. Since the latter is fixed, the total amplitude depends on four parameters.

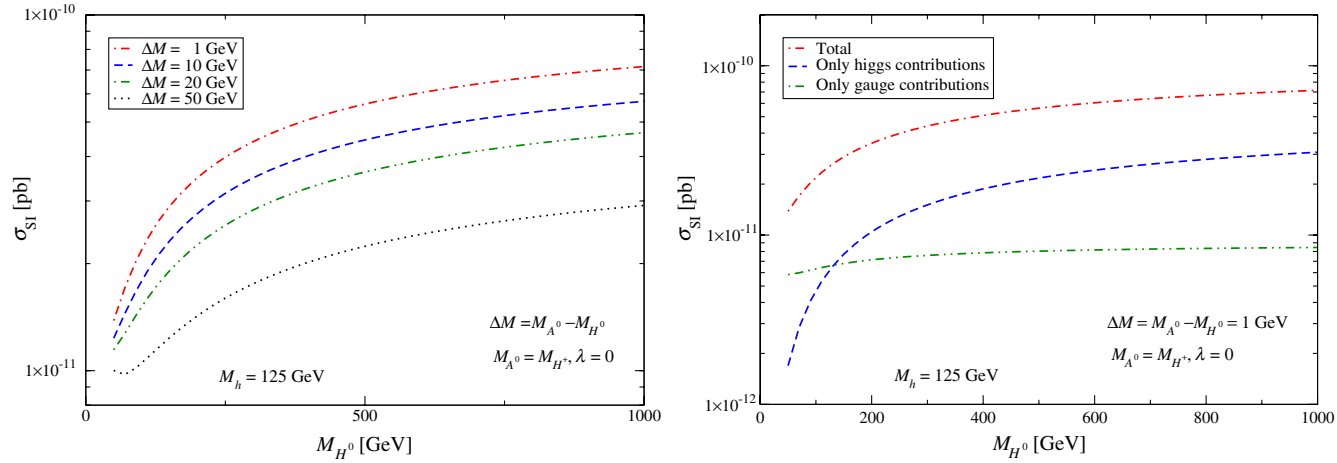

FIG. 2 (color online). Left: The purely one-loop contribution to the spin-independent cross section as a function of the dark matter mass for four different values of $\Delta M = M_{A^0}$-$M_{H^0} = M_{H^\pm}$-M_{H^0}: 1, 10, 20, and 50 GeV (from top to bottom). Right: The gauge (diagrams 1 to 6 in Fig. 1) and Higgs (last two diagrams in Fig. 1) contributions to the spin-independent cross section as a function of the dark matter mass for $\Delta M = 1$ GeV. In this figure we have set $\lambda = 0$ and $M_h = 125$ GeV.

contribution dominates whereas at high masses the Higgs contribution is more relevant. In any case, as demonstrated by the difference between the total $\sigma_{\rm SI}$ and those obtained for the Higgs and gauge contributions, neither contribution becomes negligible in the region of interest to us, so both must be taken into account in the evaluation of the spin-independent cross section.

It is also interesting to look at the behavior of $\sigma_{\rm SI}$ as a function of M_{A^0} (or $M_{H^\pm}$) for a fixed value of the dark matter mass. In Fig. 3 we illustrate that for the low mass regime ($M_{H^0} = 70$ GeV, left panel) and the heavy mass regime ($M_{H^0} = 600$ GeV, right panel). In each panel two different values of $M_{H^\pm}$ are considered. In both regimes we find that $\sigma_{\rm SI}$ decreases with M_{A^0} and with $M_{H^\pm}$ and that it varies approximately between 10^{-11} pb and 10^{-10} pb, as found before. The difference in the magnitude of $\sigma_{\rm SI}$ between the low and the large mass regime is due to the dominance of the gauge diagrams in the former case and the Higgs diagrams in the latter one.

So far in our analysis we have made two important simplifications: (i) we have set $\lambda = 0$, or equivalently we have limited ourselves to the purely one-loop contribution; (ii) we have not yet enforced the constraints on the parameters of the inert doublet model. In the next two sections, where our main results are presented, we will get rid of these simplifications. Ultimately, what we actually want to know is how important these electroweak corrections are within the viable regions of the inert doublet model. In particular, we would like to determine if they can give the dominant contribution to $\sigma_{\rm SI}$ and in which regions that happens. We also want to know how these corrections modify the prospects for the direct detection of dark matter in future experiments. To that end, we should move away from the $\lambda = 0$ limit considered in this section

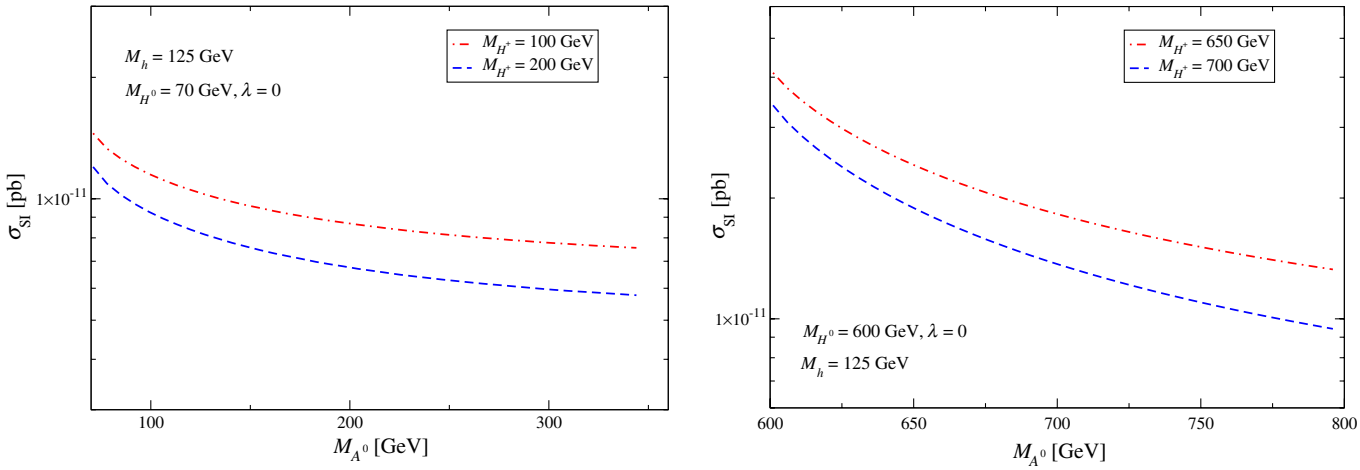

FIG. 3 (color online). The purely one-loop contribution to the spin-independent cross section as a function of M_{A^0} for different sets of parameters. In the left panel, we consider a light dark matter particle, $M_{H^0} = 70$ GeV, and $M_{H^\pm} = 100, 200$ GeV. In the right panel, a heavy dark matter candidate is considered, $M_{H^0} = 600$ GeV, and $M_{H^\pm} = 650, 700$ GeV. In both panels, $\lambda = 0$ and $M_h = 125$ GeV.

and we should ensure that $\sigma_{\rm SI}$ is evaluated only for models that are compatible with all the known phenomenological and cosmological constraints.

IV. RESULTS FOR THE LOW MASS REGIME

In this section, we examine the implications of the electroweak corrections to $\sigma_{\rm SI}$ within the low mass regime of the inert doublet model. To begin with, we show, in the left panel of Fig. 4, the viable parameter space in the plane (M_{H^0}, λ) for $M_{H^\pm} = M_{H^0} + 50$ GeV and two different values of M_{A^0}-M_{H^0}: 10 GeV and 50 GeV. Along the lines, the dark matter relic density is compatible with current observations, $\Omega h^2 = 0.11$. Since coannihilation effects are important for $M_{A^0} = M_{H^0} + 10$ GeV (dash-dotted line) the required value of λ is always smaller than that for $M_{A^0} = M_{H^0} + 50$ GeV (dashed line), where they are not. Close to the Higgs resonance, $M_{H^0} = M_h/2 = 62.5$ GeV, the annihilation of dark matter tends to be very efficient, so λ has to be very small to avoid depleting the abundance of dark matter in the early Universe. For $M_{H^0} \sim 70$–72 GeV, the annihilation into the three-body final state WW^* [20], a process dominated by the gauge interactions, is sufficient to account for the observed dark matter so λ must be small to suppress the additional Higgs-mediated annihilations (whose strength increases with λ). The main lesson from this figure is that there are regions in the viable parameter space of the inert doublet model where the scalar coupling λ is indeed much smaller than the gauge couplings, reaching values as low as 10^{-4}.

In such regions, we expect the one-loop corrections to modify in a significant way the prediction of the inert Higgs direct detection cross section, and perhaps to give a contribution larger than the tree-level one. To illustrate the effect of the electroweak corrections, in the following we will either compare $\sigma_{\rm SI}$(tree level) with $\sigma_{\rm SI}$(one loop) in the same figure or study their ratio as a function of the parameters of the model.

The right panel of Fig. 4 shows the ratio $\sigma_{\rm SI}$(one loop)/$\sigma_{\rm SI}$(tree level) along the viable lines from the left panel. As expected, the correction is large where λ is small and vice versa. We see that the one-loop correction can indeed be much larger than the tree-level result, with $\sigma_{\rm SI}$(one loop)/$\sigma_{\rm SI}$(tree level) reaching values as high as $\sim$30 for $M_{H^0} \sim 71$ GeV and $\sim$100 for $M_{H^0} \sim M_h/2$. Outside these regions, the correction is small but not necessarily negligible and may easily account for a 20% increase in $\sigma_{\rm SI}$.

A direct comparison between $\sigma_{\rm SI}$(one loop) and $\sigma_{\rm SI}$(tree level) is shown in Fig. 5. Here, we have selected, from the two viable lines discussed in the previous figure, the one featuring $M_{A^0} = M_{H^0} + 50$ GeV. For illustration, the current bound from XENON100 and the expected sensitivity of XENON-1T are also displayed. The former already excludes the regions $M_{H^0} > 53$ GeV and $64 < M_{H^0}/\text{GeV} < 70$ in this parameter space. The effect of the one-loop corrections is clearly seen close to the Higgs resonance, where it prevents the cross section from going below about 10^{-11} pb. A similar effect takes place also at the largest allowed value of M_{H^0}.

One may be tempted to conclude, from the above figures, that in the low mass regime the one-loop corrections to $\sigma_{\rm SI}$ can become very large only around two specific values of M_{H^0}, $M_h/2$, and 71 GeV, and that they are much smaller everywhere else. That such a conclusion is wrong—is only an artifact of the specific slice of the parameter space being displayed—is demonstrated by Fig. 6. Its left panel shows the viable regions for $\lambda = 10^{-2}$, 10^{-3}, 10^{-4} and $M_{H^\pm} = M_{H^0} + 50$ GeV. Because in this case H^0-A^0 coannihilations play a prominent role

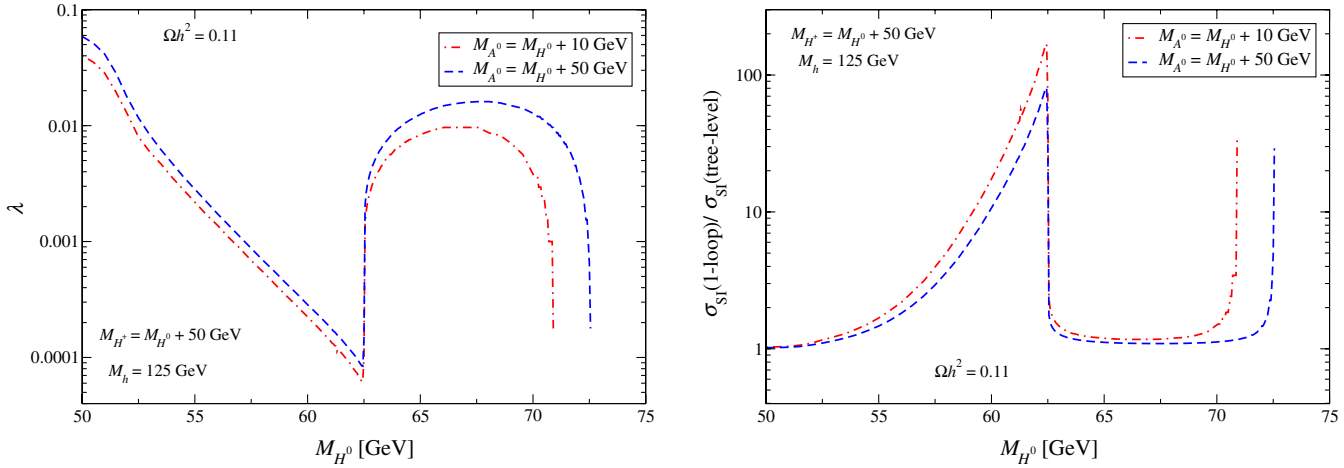

FIG. 4 (color online). Left: The viable parameter space of the inert doublet model in the plane (M_{H^0}, λ) for two different values of M_{A^0}-M_{H^0}: 10 GeV (dotted-dashed line) and 50 GeV (dashed line). In this figure, $M_{H^\pm}$-M_{H^0} was set to 50 GeV and M_h to 125 GeV. Along the lines, the dark matter constraint, $\Omega h^2 = 0.11$, is satisfied. Notice that the coupling λ can reach values as small as 10^{-4}. Right: The correction to the spin-independent direct detection cross section as a function of the dark matter mass along the viable regions from the left panel.

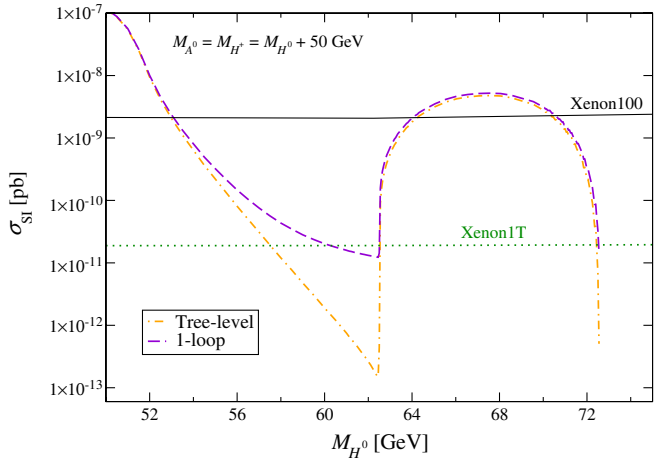

FIG. 5 (color online). A comparison between the tree-level and the one-loop direct detection cross section for one of the viable regions of Fig. 4.

in obtaining the right value of the dark matter density, it makes sense to display the parameter space in the plane (M_{H^0}, M_{A^0}-M_{H^0}). For $\lambda = 10^{-4}$ (dash-dotted line) it is always possible to find a value of M_{A^0}-M_{H^0} that gives the observed value of the dark matter density, but that is not true for $\lambda = 10^{-3}$ or $\lambda = 10^{-2}$. Notice that the required mass splitting increases significantly close to the Higgs resonance and near the maximum allowed value of M_{H^0}. The small bump observed at $M_{H^0} \sim 52.5$ GeV is due to the effect of resonant A^0-A^0 annihilations on the relic density. The right panel of Fig. 6 shows the correction to σ_{SI} along such viable regions. We see that in this case the correction does not strongly depend on M_{H^0}: it is of order of several percent for $\lambda = 10^{-2}$ (solid line), a factor 2 to 4 for $\lambda = 10^{-3}$ (dashed line), and it reaches almost a factor 100 for $\lambda = 10^{-4}$ (dash-dotted line). In all cases there is a slight increase in the correction with the dark matter mass. Clearly, large electroweak corrections to σ_{SI} are not confined to $M_{H^0} \sim M_h/2$ and $M_{H^0} \sim 70$ GeV but can actually be found for any value of M_{H^0}. At the end, it is the size of λ and not M_{H^0} that determines how important the corrections are, and λ can vary over several orders of magnitude within the viable regions of the model.

To assess in all generality, and independently of the specific slice of parameter space examined, the relevance of the electroweak corrections to σ_{SI}, we have scanned, using Markov chain Monte Carlo techniques [34], the entire parameter space of the inert doublet model. After allowing the parameters to vary within the following ranges

$$80 \text{ GeV} > M_{H^0} > 50 \text{ GeV}, \tag{6}$$

$$M_{A^0} > M_{H^0}, \tag{7}$$

$$M_{H^\pm} > 90 \text{ GeV}, \tag{8}$$

$$1 > \lambda > 10^{-5}, \tag{9}$$

and imposing all the experimental bounds (collider, precision, dark matter, etc.), we obtained a sample of about 10^4 viable models to analyze. Figure 7 shows a scatter plot of these models in the plane (M_{H^0}, σ_{SI}). The (blue) squares show σ_{SI}(tree level) and the (red) circles σ_{SI}(one loop). Two classes of models can be easily distinguished in this figure: the *annihilating* models that are concentrated along a narrow band similar to that observed in Fig. 5 and the *coannihilating* models that are scattered in the region below that band. They are absent below $M_{H^0} \sim 55$ GeV

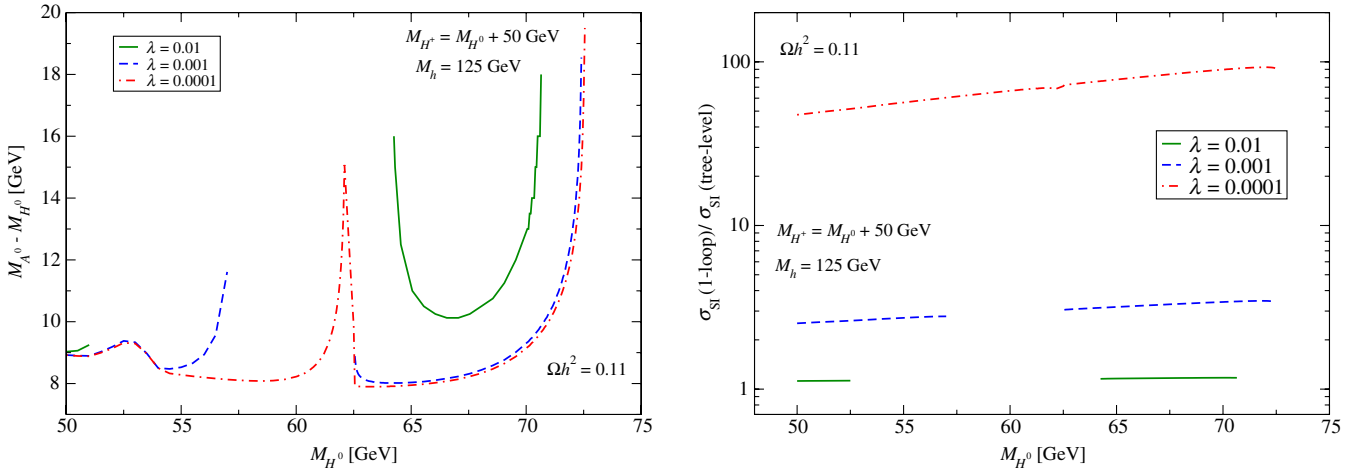

FIG. 6 (color online). Left: The parameter space of the inert doublet model in the plane (M_{H^0}, M_{A^0}-M_{H^0}) for three different values of the coupling λ: 10^{-2} (solid line), 10^{-3} (dashed line), and 10^{-4} (dashed-dotted line). The value of $M_{H^\pm}$ was set to $M_{H^0} + 50$ GeV. Along the lines the relic density constraint, $\Omega h^2 = 0.11$, is satisfied—mainly via H^0-A^0 coannihilations. Notice that for $\lambda = 10^{-2}$ and $\lambda = 10^{-3}$ there is a range in M_{H^0} with no viable points. Right: The correction to the spin-independent direct detection cross section as a function of the dark matter mass along the viable lines from the left panel. Notice that in this case the correction only slightly depends on M_{H^0}.

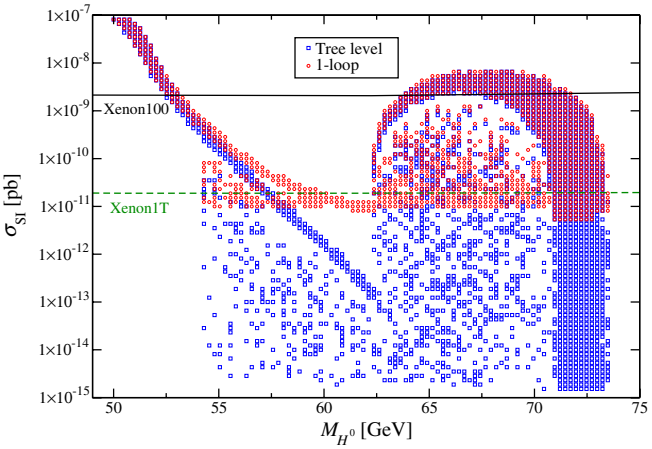

FIG. 7 (color online). A scatter plot of the spin-independent direct detection cross section at tree level and at one loop as a function of the dark matter mass. In this figure all the parameters of the inert Higgs model were allowed to vary randomly (see text for details) and all experimental bounds were taken into account.

because the mass splitting required for coannihilations to be important becomes inconsistent with collider bounds [12]. Notice that whereas σ_{SI}(tree level) may be as small as 10^{-15} pb, σ_{SI}(one loop) does not go below 10^{-11} pb or so. From the figure we also see that some regions are already excluded by the XENON100 bound [3] (solid line). The most important result, however, is the fact that the one-loop corrections always bring σ_{SI} within the reach of future direct detection experiments and, in particular, very close to the XENON-1T expected sensitivity.

Figure 8 shows the same sample of viable models, but in two additional planes. The right panel shows σ_{SI}(one loop)/σ_{SI}(tree level) as a function of M_{H^0}. The annihilating and coannihilating models can again be clearly distinguished in this figure. Notice that the correction can be very large, say σ_{SI}(one loop)/σ_{SI}(tree level) $\sim$ 100, pretty much for any value of M_{H^0}. The right panel displays the same ratio but now as a function of λ. The general behavior is as anticipated, with the correction increasing for decreasing λ. It can also be seen in this figure that σ_{SI}(one loop) becomes larger than σ_{SI}(tree level) for $\lambda \gtrsim 10^{-3}$, as we had found before. The small spread observed in this figure clearly demonstrates that it is the size of λ that determines how large σ_{SI}(one loop)/σ_{SI}(tree level) is.

Summarizing, we have seen that in the small mass regime of the inert doublet model, $M_{H^0} < M_W$, the electroweak corrections to the spin-independent direct detection cross section can be quite relevant, giving in certain cases the dominant contribution to σ_{SI}. We have observed that these corrections become large when $\lambda \lesssim 10^{-3}$. Such values of λ are compatible with the dark matter constraint thanks to coannihilations (for a wide range of M_{H^0}), resonant annihilations (for $M_{H^0} \lesssim M_h/2$), or annihilations into three-body final states (for $M_{H^0} \sim 72$ GeV). We have also noticed that in contrast to σ_{SI}(tree level), which can be arbitrarily small, σ_{SI}(one loop) is never below $\sim 10^{-11}$ pb. Thus, over the entire low mass regime, the electroweak corrections we have studied bring σ_{SI} within the reach of future direct detection experiments.

V. RESULTS FOR THE LARGE MASS REGIME

We now focus our attention on the heavy mass regime of the model, $M_{H^0} \gtrsim 500$ GeV. Figure 9 shows viable regions of the inert doublet model in the plane (M_{H^0}, M_{A^0}-M_{H^0}) for different values of the scalar coupling λ. For concreteness, in this figure we have set $M_{H^\pm} = M_{A^0}$ and we have restricted the mass range to $M_{H^0} < 1$ TeV. Notice that even though the mass splitting between the inert particles increases with the dark matter mass, it is always very small (below the percent level). At $M_{H^0} =$ 1 TeV, for instance, it amounts to no more than 7 GeV. This is a generic and well-known feature of the large mass

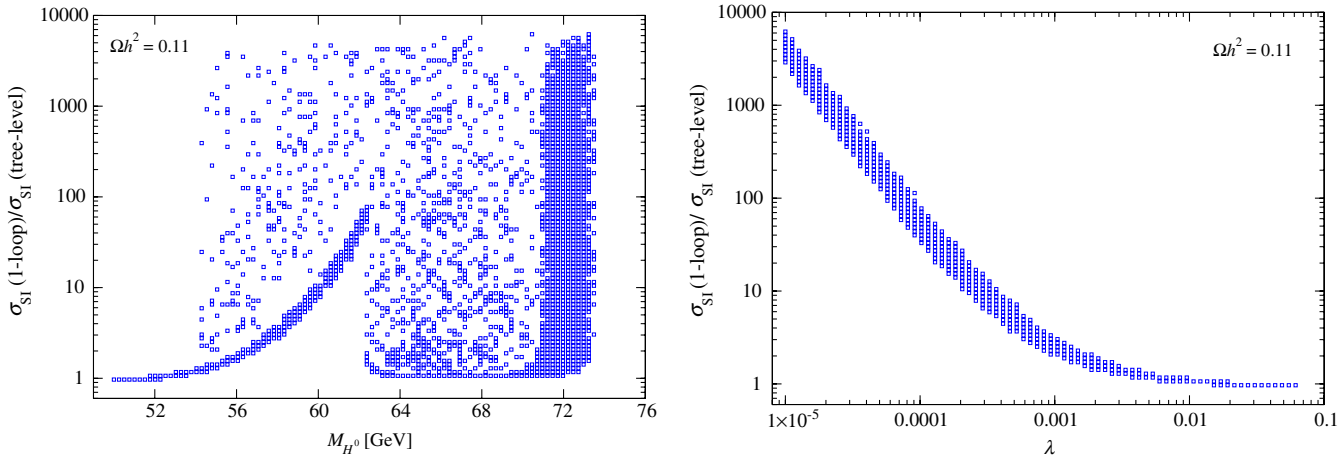

FIG. 8 (color online). Left: A scatter plot of σ_{SI}(one loop)/σ_{SI}(tree level) as a function of M_{H^0}. Right: A scatter plot of σ_{SI}(one loop)/σ_{SI}(tree level) as a function of λ. In this figure all the parameters of the inert Higgs model were allowed to vary randomly (see text for details) and all experimental bounds were taken into account.

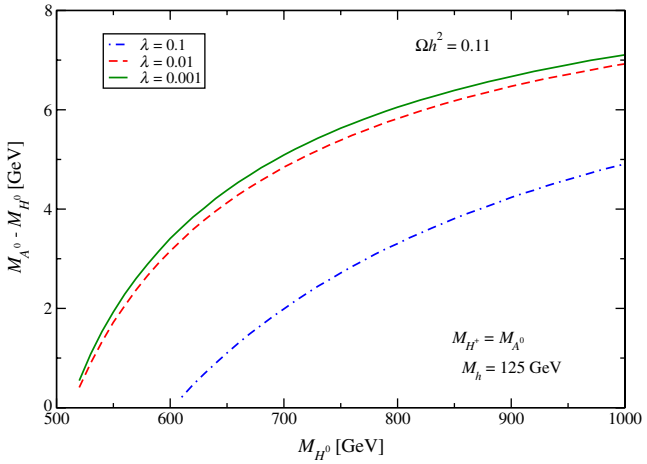

FIG. 9 (color online). The viable parameter space of the inert doublet model in the plane (M_{H^0}, M_{A^0}-M_{H^0}) for different values of λ. In this figure we consider the large mass regime of the model and we set $M_{H^\pm} = M_{A^0}$ and $M_h = 125$ GeV. Notice that the required mass splitting is always very small.

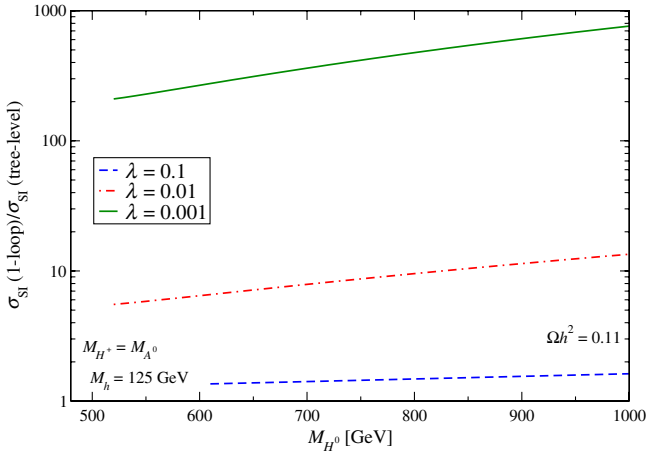

FIG. 10 (color online). The correction to the spin-independent direct detection cross section as a function of the dark matter mass along the viable lines of Fig. 9.

regime of the inert doublet model: only for small values of M_{A^0}-M_{H^0} and $M_{H^\pm}$-M_{H^0} can the relic density constrained be satisfied, see e.g., Ref. [33]. In the figure we see that the viable parameter space starts at $M_{H^0} \sim 520$ GeV for $\lambda = 10^{-2}$, 10^{-3} and around 600 GeV for $\lambda = 0.1$. In this regime there are neither resonances nor thresholds, so the analysis is much simpler. As we saw in Fig. 2, the one-loop correction to $\sigma_{\rm SI}$ initially increases with M_{H^0} whereas the tree-level value of $\sigma_{\rm SI}$ decreases with $M_{H^0}^2$ [see Eq. (5)]. Since, in addition, λ can be made arbitrarily small in this regime, we expect that the electroweak corrections to $\sigma_{\rm SI}$ be more relevant than for the low mass regime. Figure 10 shows $\sigma_{\rm SI}$(one loop)/$\sigma_{\rm SI}$(tree level) along the viable lines of Fig. 9. As expected, the correction is larger the smaller λ is. We also observe that as M_{H^0} increases, the correction indeed becomes more important. It amounts to a factor between 1 and 2 for $\lambda = 0.1$, about a factor 10 for $\lambda = 0.01$, and more than 200 for $\lambda = 10^{-3}$. Notice, for example, that in the large mass regime $\sigma_{\rm SI}$(one loop)/$\sigma_{\rm SI}$(tree level) ~ 2 can be obtained already for $\lambda = 0.1$ whereas in the low mass regime that would require a value of λ at least 1 order of magnitude smaller.

We have also scanned the parameter space of this regime by allowing the inert masses to vary in the range

$$1 \text{ TeV} > M_{H^0} > 500 \text{ GeV}, \tag{10}$$

$$M_{H^\pm} > M_{H^0}, \tag{11}$$

$$M_{A^0} > M_{H^0}. \tag{12}$$

After imposing all the relevant constraints, we obtained a sample of approximately 10^4 viable models. Figure 11

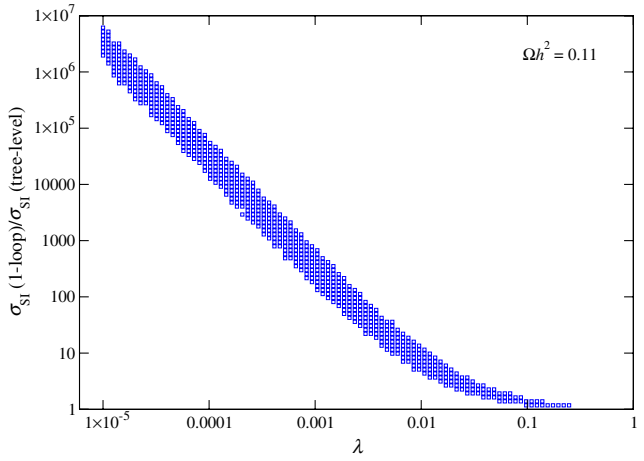

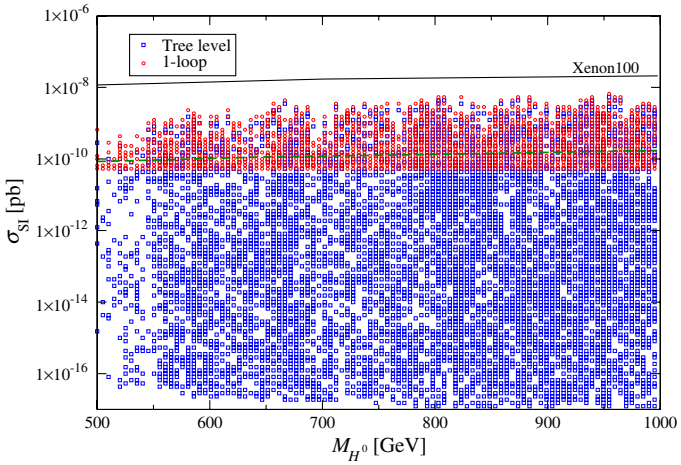

FIG. 11 (color online). Some results of the scan over the parameters of the model for the large mass regime. Left: A scatter plot of the correction to $\sigma_{\rm SI}$ as a function of λ. Right: A comparison between the tree-level and the one-loop value of $\sigma_{\rm SI}$ as a function of M_{H^0}. The solid line shows the current bound from XENON100 whereas the dashed line corresponds to the expected sensitivity of XENON-1T.

shows this sample of models in two different planes. The left panel displays $\sigma_{\rm SI}(\text{one loop})/\sigma_{\rm SI}(\text{tree level})$ as a function of λ. It demonstrates that $\sigma_{\rm SI}(\text{one loop})/\sigma_{\rm SI}(\text{tree level})$ is a decreasing function of λ, as expected and that it becomes much larger than 1, say ~ 10, for $\lambda \sim 10^{-2}$. The small spread of models in this plane again indicates that it is fundamentally λ the parameter that determines the size of $\sigma_{\rm SI}(\text{one loop})/\sigma_{\rm SI}(\text{tree level})$. The right panel compares the tree-level and one-loop values of $\sigma_{\rm SI}$ as a function of M_{H^0}. Notice that whereas at tree level $\sigma_{\rm SI}$ could be as small as 10^{-17}pb, at one loop it is never below 10^{-11} pb. From the figure we see that this region is not being currently probed by direct detection experiments—see the present XENON100 bound (solid line). The future prospects, however, are very good because the one-loop corrections bring $\sigma_{\rm SI}$ within the reach of planned direct detection experiments.

VI. CONCLUSIONS

We have computed and studied the dominant electroweak corrections to the direct detection cross section of inert Higgs dark matter. These corrections arise from one-loop diagrams mediated by the electroweak gauge bosons and do not depend on the scalar coupling λ that controls the tree-level cross section. We have analyzed the behavior of these one-loop contributions as a function of the parameters of the model, and have calculated their effect within the regions that are compatible with the dark matter constraint for the two distinct regimes of this model: the low mass regime ($M_{H^0} < M_W$) and the large mass regime ($M_{H^0} \gtrsim 500$ GeV). In both regimes, we have found regions where the one-loop corrections not only become significant but can even be larger than the tree-level result. In the low mass regime, this happens when $\lambda \lesssim 10^{-3}$, a value that can be compatible with the dark matter constraint via annihilation through the Higgs resonance, annihilation into the three-body final state WW^*, or coannihilations. The first two require, respectively, $M_{H^0} \sim M_h/2$ and $M_{H^0} \sim 72$ GeV whereas coannihilations allow for a much wider range of M_{H^0}. In the heavy mass regime, we found the effect of the electroweak corrections to be larger, with corrections of order 100% already for $\lambda = 0.1$. Thus, they must be necessarily taken into account when assessing the prospects for the direct detection of inert Higgs dark matter. From the scans over the full parameter space of the model, we also observed that these one-loop contributions always bring $\sigma_{\rm SI}$ within the reach of future direct detection experiments.

ACKNOWLEDGMENTS

We would like to thank M. Gustafsson for pointing out an error in Figs. 2 and 3 of a previous version of this manuscript. This work is supported by the "Helmholtz Alliance for Astroparticle Phyics HAP" funded by the Initiative and Networking Fund of the Helmholtz Association. J. D. R. would like to thank D. Restrepo for his collaboration.

[1] E. Komatsu *et al.*, Astrophys. J. Suppl. Ser. **192**, 18 (2011).
[2] E. Aprile *et al.*, Astropart. Phys. **35**, 573 (2012).
[3] E. Aprile *et al.*, Phys. Rev. Lett. **109**, 181301 (2012).
[4] M. Farina, M. Kadastik, D. Pappadopulo, J. Pata, M. Raidal, and A. Strumia, Nucl. Phys. **B853**, 607 (2011).
[5] C. Strege, G. Bertone, D. G. Cerdeño, M. Fornasa, R. Ruiz de Austri, and R. Trotta, J. Cosmol. Astropart. Phys. 03 (2012) 030.
[6] Y. Mambrini, Phys. Rev. D **84**, 115017 (2011).
[7] A. Melfo, M. Nemevsek, F. Nesti, G. Senjanovic, and Y. Zhang, Phys. Rev. D **84**, 034009 (2011).
[8] R. Barbieri, L. J. Hall, and V. S. Rychkov, Phys. Rev. D **74**, 015007 (2006).
[9] E. Ma, Phys. Rev. D **73**, 077301 (2006).
[10] L. L. Honorez, E. Nezri, J. F. Oliver, and M. H. G. Tytgat, J. Cosmol. Astropart. Phys. 02 (2007) 028.
[11] M. Gustafsson, E. Lundstrom, L. Bergstrom, and J. Edsjo, Phys. Rev. Lett. **99**, 041301 (2007).
[12] E. Lundstrom, M. Gustafsson, and J. Edsjo, Phys. Rev. D **79**, 035013 (2009).
[13] P. Agrawal, E. M. Dolle, and C. A. Krenke, Phys. Rev. D **79**, 015015 (2009).
[14] S. Andreas, M. H. G. Tytgat, and Q. Swillens, J. Cosmol. Astropart. Phys. 04 (2009) 004.
[15] E. M. Dolle and S. Su, Phys. Rev. D **80**, 055012 (2009).
[16] E. Nezri, M. H. G. Tytgat, and G. Vertongen, J. Cosmol. Astropart. Phys. 04 (2009) 014.
[17] C. Arina, F.-S. Ling, and M. H. G. Tytgat, J. Cosmol. Astropart. Phys. 10 (2009) 018.
[18] E. Dolle, X. Miao, S. Su, and B. Thomas, Phys. Rev. D **81**, 035003 (2010).
[19] X. Miao, S. Su, and B. Thomas, Phys. Rev. D **82**, 035009 (2010).
[20] L. L. Honorez and C. E. Yaguna, J. High Energy Phys. 09 (2010) 046.
[21] L. L. Honorez and C. E. Yaguna, J. Cosmol. Astropart. Phys. 01 (2011) 002.
[22] B. Grzadkowski, O. M. Ogreid, P. Osland, A. Pukhov, and M. Purmohammadi, J. High Energy Phys. 06 (2011) 003.
[23] H. Martinez, A. Melfo, F. Nesti, and G. Senjanovic, Phys. Rev. Lett. **106**, 191802 (2011).
[24] T. A. Chowdhury, M. Nemevsek, G. Senjanovic, and Y. Zhang, J. Cosmol. Astropart. Phys. 02 (2012) 029.

[25] D. Borah and J. M. Cline, Phys. Rev. D **86**, 055001 (2012).
[26] M. Gustafsson, S. Rydbeck, L. Lopez-Honorez, and E. Lundstrom, Phys. Rev. D **86**, 075019 (2012).
[27] A. Arhrib, R. Benbrik, and N. Gaur, Phys. Rev. D **85**, 095021 (2012).
[28] G. Aad *et al.*, Phys. Lett. B **716**, 1 (2012).
[29] S. Chatrchyan *et al.*, Phys. Lett. B **716**, 30 (2012).
[30] A. Pierce and J. Thaler, J. High Energy Phys. 08 (2007) 026.
[31] G. Belanger, F. Boudjema, P. Brun, A. Pukhov, S. Rosier-Lees, P. Salati, and A. Semenov, Comput. Phys. Commun. **182**, 842 (2011).
[32] M. Cirelli, N. Fornengo, and A. Strumia, Nucl. Phys. **B753**, 178 (2006).
[33] T. Hambye, F.-S. Ling, L. L. Honorez, and J. Rocher, J. High Energy Phys. 07 (2009) 090.
[34] E. A. Baltz and P. Gondolo, J. High Energy Phys. 10 (2004) 052.